Research article

# Theoretical predication of temperature effects at 20$^o$C–42$^o$C on adaptive processes in simulated amyotrophic lateral sclerosis

D. I. Stephanova[1,*] and A. Kossev[1]

[1] *Institute of Biophysics and Biomedical Engineering, Bulgarian Academy of Sciences, Acad. G. Bontchev Str. Bl 21, Sofia 1113, Bulgaria*

*__Correspondence__: dsteph@bio.bas.bg (D. I. Stephanova)

https://doi.org/10.31083/j.jin.2018.04.0417

**Abstract**

Strength-duration time constants, rheobase currents, and recovery cycles allow the nerve adaptive processes to single or pairs of depolarizing stimuli to be assessed. This study investigates the temperature dependence of these excitability indices of human motor nerve fibers with one of three increasingly-severe type of amyotrophic lateral sclerosis pathology, referred to as ALS1, ALS2, and ALS3. The temperature dependence of the excitability indices was investigated during hypothermia ($\leq$ 25$^o$C), hyperthermia ($\geq$ 40$^o$C), and in the physiological temperature range (30–37$^o$C). Numerical solutions were computed using a temperature-dependent multi-layered model. Results showed the following trends: (i) while the strength-duration time constants gradually decreased with a temperature increase from 20$^o$C to 42$^o$C, they were longer in the three ALS cases than those of the normal case; (ii) the reciprocally dependent strength-duration time constants and rheobase currents were more sensitive to hyperthermia, especially at 42$^o$C, than at temperatures across the physiological range of 30–37$^o$C; (iii) the shape of temperature-dependent recovery cycles was similar for both the normal and ALS1 cases; (iv) in the ALS2 case, each test stimulus applied at the end of 100 ms recovery cycle failed to initiate a second action potential during hypothermia at 20$^o$C; and (v) in the ALS3 case during hypothermia, hyperthermia and across the physiological temperature range, each test stimulus applied beyond a given conditioning-test interval was blocked. This blockage was a result of the spontaneous action potential generation caused by the conditioning (first) stimulus. The changes obtained for the temperature-dependent strength-duration time constants, rheobase currents, and recovery cycles reflect nodal and internodal ion channel dysfunctions in the three amyotrophic lateral sclerosis cases. It is proposed that these excitability indices can be applied clinically as specific indicators for amyotrophic lateral sclerosis motor neuron disease.

*Keywords*

Temperature, myelinated axons, ALS, strength-duration time constant, rheobase current, recovery cycle, computational neuroscience

**Submitted:** September 14, 2017; **Accepted:** February 23, 2018

## 1. Introduction

Amyotrophic lateral sclerosis (ALS) is a usually fatal disorder causing progressive death of the motor neurons in both the cerebral cortex and the spinal cord. The pathological mechanisms of upper and lower motor neuron degeneration in this disorder have not been fully elucidated. ALS is a progressively debilitating disease characterized by increasing skeletal muscle atrophy starting in the limbs and spreading to the rest of the body [1–3], often accompanied by widespread fasciculations [4–12], possibly suggesting motor nerve axonal hyperexcitability [4, 7, 12, 13]. There is also the theory that these fasiculations are due the spreading of acetylcholine (ACh) receptors over the muscle surface: denervation hypersensitivity.

A threshold tracking technique [14–17] has been clinically employed to assess nerve adaptation in control subjects [18, 19] and patients with neurological disorders including and three progressively greater degrees of ALS severity (at or above a skin temperature of 32$^o$C) referred to as ALS1, ALS2, and ALS3 [20–27]. In those studies, the following excitability parameters were measured: strength-duration curves, charge-duration curves, strength-duration time constants, rheobase currents, refractoriness, superexcitability, and late subexcitabiliy in a 100 ms recovery cycle. The same excitability indices have previously been simulated for the three ALS classes at normal temperature (37$^o$C [28, 29]). These studies showed that in comparison to the normal case, the strength-duration time constants gradually increase and the rheobase currents gradually decrease in the gradually increasingly severe ALS1 and ALS2 cases. No differences were obtained for strength-duration time constants and rheobase currents for ALS2 and ALS3 cases. Recovery cycles showed that the excitability changes of normal and abnormal ALS axons are particularly different. The ALS1 axon has a shorter refractoriness, greater superexcitability (or supernormality), and late subexcitability than for those of the normal one. In the ALS2 case, superexcitability increases markedly and the axon remains superexcitable to the end of the tested period. In the ALS3 case, the superexcitability increases rapidly and abnormalities are obtained in the recovery cycle beyond a 50 ms conditioning-test interval. In this case, a block of each test stimulus applied to the internodal axolemma is the result of the spontaneous axonal activities caused

  

by the conditioning action potential.

Temperature effects on adaptive processes have also been examined in the range of 20–42$^o$C in simulated human motor nerve axons [30]. The temperature effects on adaptive processes in the cases of ALS1, ALS2, and ALS3 were investigated and analyzed across the same range of temperatures in the present study. Results showed that in these ALS cases as in the normal case, the strength-duration time constants and rheobase currents were more sensitive to hypothermia ($\leq 25^o$C) and most sensitive to hyperthermia ($\geq 40^o$C), especially at 42$^o$C, than for temperatures across the physiological range (30–37$^o$C). Results also showed that for both the normal and the three abnormal ALS cases, with a temperature increase from 20$^o$C to 42$^o$C the axonal superexcitability in a 100 ms recovery cycle was complex. It will be shown that such temperature-dependent changes obtained in the investigated excitability indices reflect axonal ion channel dysfunctions and membrane potential in the three ALS cases.

## 2. Methods

The simulations presented here were performed using a temperature-dependent multi-layered numerical model of human motor nerve fibres developed by the authors. The control (normal) temperature was 37$^o$C ([31, 32]; see [33, 34] for detailed descriptions of this model). Results due to temperature variations were computed by changing the temperature coefficients ($Q_{10}$-values; see Appendix of [35]) for both the ionic currents (nodal, internodal) and the geometry-independent conductivities of axoplasm and periaxonal space. The equilibrium potential values were also temperature ($T$) corrected (i.e. $RT/F$ where R is the universal gas constant and F is the Faraday constant). The $Q_{10}$'s and related details were also thoroughly described and discussed. The myelin sheath was represented as a series of 150 parallel interconnecting lamellae with 150 lipid and 150 aqueous layers. The model axon consisted of 30 nodes and 29 internodes. Each internode was sub-divided into two paranodal and five internodal segments. The lengths of node, paranode, and nodal center to nodal center were 1.5, 200 and 1400 $\mu$m, respectively. All calculations were carried out for fibers with an axon diameter of 12.5 $\mu$m, an external fibre diameter of 17.3 $\mu$m, with a conduction velocity of 61.25 m/sec. All other parameters were as previously given [31, 32].

This temperature-dependent, multi-layered model was applied to the previously simulated ALS1, ALS2, and ALS3 cases [28, 29]. The uniform axonal dysfunctions of active parameters such as maximum permeabilities of nodal and internodal ion channels with their characteristic values follow those suggested by Bostock *et al.* [20]. Specifically they were: (i) nodal fast potassium ($K_f^+$) channels were blocked in the ALS1 case, i.e. $P_{Kf} = 0$, (ii) nodal slow potassium ($K_s^+$) and internodal fast potassium ($K_f^+$) channels were blocked in the ALS2 case, i.e. $P_{Ks} = 0$ and $P^*_{Kf} = 0$, and (iii) nodal slow ($K_s^+$), internodal fast ($K_f^+$), and slow ($K_s^+$) potassium channels were blocked in the ALS3 case, i.e. $P_{Ks} = 0$, $P^*_{Kf} = 0$, and $P^*_{Ks} = 0$. The *asterisk* denotes an internodal quantity. Also, the values of passive parameters such as axoplasmic resistance ($R_{ax}$), paranodal seal resistance ($R_{pn}$), and remaining active parameter values in the ALS1 case were adjusted to achieve near normal conduction velocity and polarizing threshold electrotonus obtained *in vivo* and *in vitro* in human motor nerve fibers at normal temperature [20]. Each increasingly-severe ALS type was simulated based on the previous type and the active parameter values were adjusted to produce: (i) action potential generation during the early part of the depolarizing electrotonic potential in the ALS2 case, and (ii) spontaneous discharge of the electronic potential after termination of the applied hyperpolarizing stimulus in the ALS3 case. These ALS pathologies were originally described at normal temperature by Bostock *et al.* [20].

Temperatures were changed concurrently and equally in each segment along the fibre length. The strength-duration curves, charge-duration curves, strength-duration time constants, rheobase currents, and recovery cycles were investigated during hypothermia ($\leq 25^o$C), hyperthermia ($\geq 40^o$C) and in the physiological range (30–37$^o$C). To study adaptation, depolarizing long-duration pulses of intracellular current were applied simultaneously at the center of each internodal segment [36] using threshold or suprathreshold amplitudes. Elicited action potentials occurred simultaneously within each nodal and internodal segment along the fibre.

For a given temperature, the threshold stimulus duration was increased in 0.025 ms steps from 0.025 ms to 1 ms for constructing the strength-duration curves. These curves were not simple single-exponential functions, and thus the associated charge-duration curves were not linear. However, the following polynomial function of second degree (transfer parabola), which related the threshold charge ($Q$) to stimulus duration ($t$), provided an accurate fit of the data: $Q = a_2[t^2 + (a_1/a_2)\cdot t + a_0/a_2]$, where $a_0$, $a_1$, and $a_2$ are the polynomial coefficients. The strength-duration time constant (chronaxie) was defined as the absolute value of the smallest square root of the function (i.e. only one of both direct intercepts of the regression curve on the duration axis has a biophysical sense and only this direct intercept is shown on the charge-duration figures). The rheobase current was defined as the final decreased threshold value, after which action potentials could not be obtained by increased stimulus duration.

For a given temperature, the test stimulus amplitude required to elicit a second action potential during the relative refractory period was either greater or less than the conditioning stimulus amplitude, depending on the conditioning test (CT) intervals. To obtain the time course of recovery of axonal excitability following a single stimulus (the recovery cycle), test threshold current stimuli of one ms duration were delivered at CT intervals of 2–100 ms after a suprathreshold conditioning current stimulus of one ms duration. The test stimulus thresholds were determined at 27 CT intervals, with the intervals being increased up to 100 ms in approximately geometric progression. Three stimulus combinations were tested: (i) conditioning (first) stimulus (duration one ms) was determined at threshold; (ii) suprathreshold conditioning stimulus (duration one ms) was calculated, which was increased by 5% of threshold, and (iii) the first suprathreshold (conditioning) plus the test (second) threshold stimuli were used to obtained the recovery cycle.

## 3. Results

### 3.1. *Abnormalities in the strength-duration time constants and rheobase currents in the ranges of 20–42$^o$C and 30–37$^o$C for the normal and three ALS cases*

Comparison of the strength-duration curves (Fig. 1, first column) and charge-duration curves (Fig. 1, last column) is shown for normal (Fig. 1a), ALS1 (Fig. 1b) and ALS2 (Fig. 1c) cases during hypothermia (20$^o$C, 25$^o$C) and hyperthermia (40$^o$C, 42$^o$C). The same parameters are shown in Fig. 2 for the physiological temperature range from 30–37$^o$C. There was no difference in these curves for

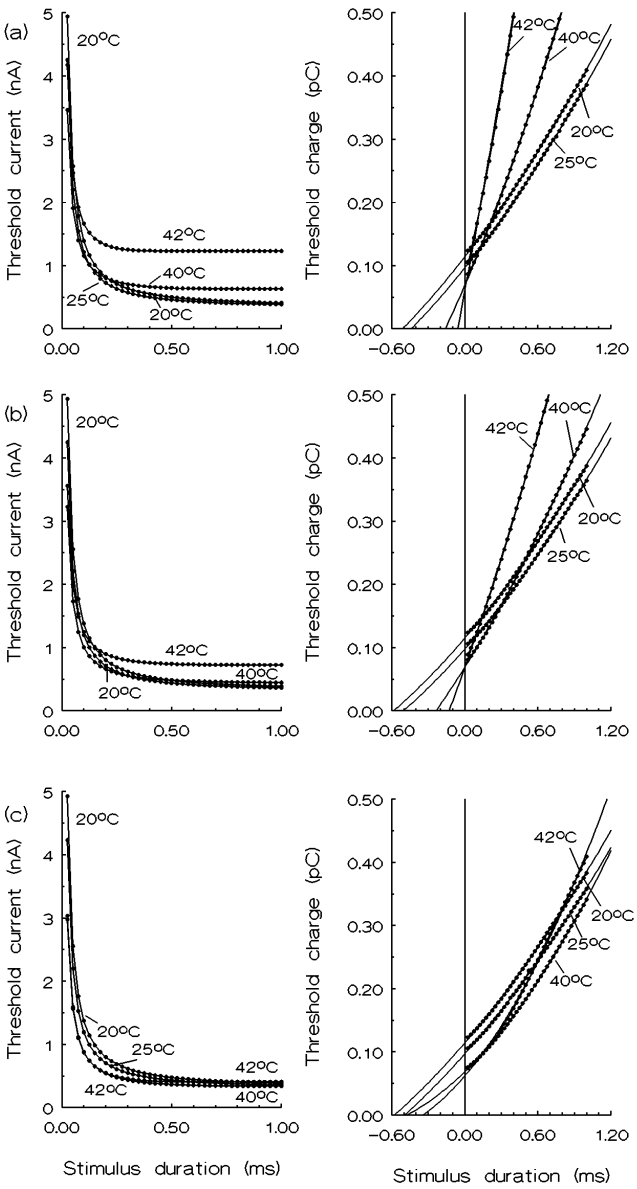


Fig. 1. Comparison between the strength-duration curves (first column) and charge-duration curves (last column) in the normal (a), ALS1 (b), and ALS2 = ALS3 (c) cases of hypothermic myelinated human motor nerve fibre (20$^o$C and 25$^o$C) and hyperthermia (40$^o$C and 42$^o$C). The strength-duration curves almost superimpose in the ALS1 case at 20$^o$C and 25$^o$C, thus lower temperature only is given.

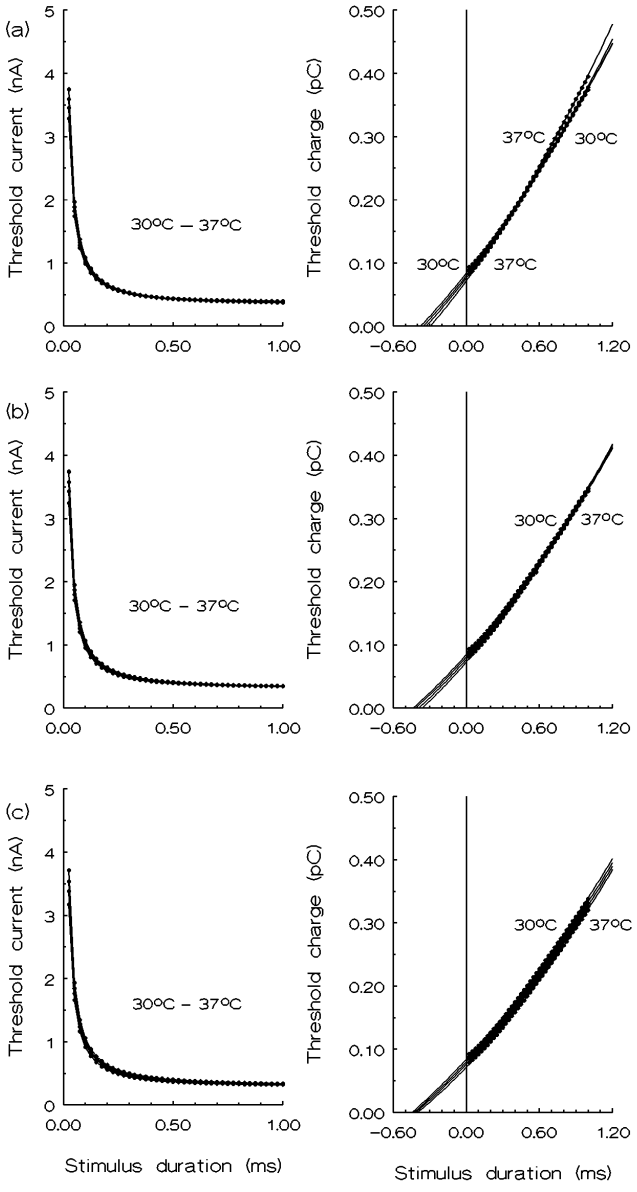


Fig. 2. Comparison between the strength-duration curves (first column) and charge-duration curves (last column) in the normal (a), ALS1 (b), and ALS2 = ALS3 (c) cases of the myelinated human motor nerve fibre in the physiological temperature range (30$^o$C, 32$^o$C, 34$^o$C, and 37$^o$C). The strength-duration and charge-duration curves almost superimpose, thus lowest and highest temperatures only are given.

the ALS2 and ALS3 cases with changes in temperature. Histograms are also given to better illustrate the strength-duration time constants (Fig. 3, first column) and rheobase currents (Fig. 3, last column) for the normal (hatched first bars, from left to right), ALS1 (white second bars), and ALS2 = ALS3 (hatched last bars) cases in the panel figures for the temperature ranges of 20–42$^o$C (Fig. 3a) and 30–37$^o$C (Fig. 3b). The strength-duration time constants for the normal/ALS1/ALS2 cases were 0.509/0.583/0.577, 0.439/0.503/0.494, 0.159/0.236/0.462 and 0.058/0.123/0.344 ms and the rheobase currents were 0.283/0.281/0.236, 0.305/0.295/0.240, 0.631/0.443/0.340 and 1.231/0.723/0.409 nA at 20$^o$C, 25$^o$C, 40$^o$C and 42$^o$C, respectively (Fig. 3a). The strength-duration time constants were longest for the normal and three ALS cases at 20$^o$C and they were shortest at 42$^o$C, while the rheobase currents were lowest at 20$^o$C and highest at 42$^o$C. Compared to the normal case, ALS1 and ALS2 = ALS3 cases had longer strength-duration time constants and lower rheobase currents. However, the strength-duration time constants and rheobase currents for the three abnormal ALS cases were most sensitive to hyperthermia ($\geq$ 40$^o$C), especially 42$^o$C, than to hypothermia ($\leq$ 25$^o$C). Consequently, the transition from 20$^o$C to 42$^o$C leads to amplification of the degree of parameter changes, as the direction of these changes is maintained.

In the almost superimposed strength-duration curves for the normal/ALS1/ALS2 cases at 30$^o$C, 32$^o$C, 34$^o$C, and 37$^o$C (Fig. 2, first

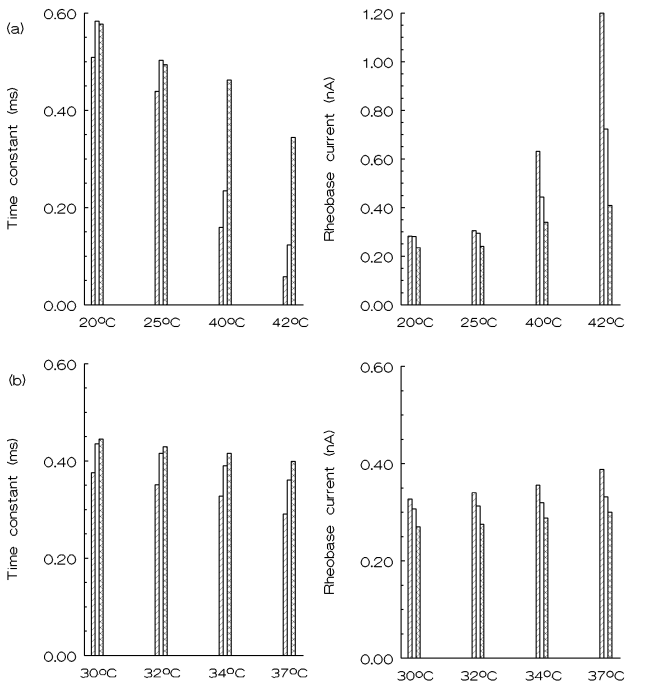


Fig. 3. Comparison between the strength-duration time constants (first column) and rheobase currents (last column) for normal (hatched first bars, from left to the right), ALS1 (white second bars), and ALS2 = ALS3 (hatched last bars) cases in the panel figures for the temperature ranges of 20–42$^o$C (a) and 30–37$^o$C (b), respectively.

column), the threshold stimulus currents were highest for the 0.025 ms stimulus and lowest for the one ms stimulus. However, for each of these normal and three ALS cases, the strength-duration time constants and rheobase currents were slightly changed with a temperature increase from 30$^o$C to 37$^o$C (Fig. 3b) when compared to those of the temperature range of 20–42$^o$C (Fig. 3a). In the physiological temperature range, there was again an inverse relationship between the strength-duration time constants and rheobase currents, where the ALS1 and ALS2 = ALS3 cases had longer strength-duration time constants and lower rheobase currents when compared with the normal case (Fig. 3b). The strength-duration time constants for the normal/ALS1/(ALS2 = ALS3) cases were 0.376/0.435/0.445, 0.351/0.416/0.429, 0.328/0.390/0.416, and 0.291/0.361/0.399 ms and the rheobase currents were 0.327/0.307/0.270, 0.340/0.313/0.275, 0.356/0.320/0.288 and 0.388/0.332/0.300 nA at 30$^o$C, 32$^o$C, 34$^o$C and 37$^o$C, respectively (Fig. 3b).

Consequently, with the increase of temperature from 20$^o$C to 40$^o$C, strength-duration time constants for the normal/ALS1/ALS2 cases decreased by a factor of 3.20/2.47/1.25 times, while they decreased by a factor of 1.15/1.12/1.07 times in the range of 30–37$^o$C. Conversely, the rheobase currents increased by a factor of 2.23/1.58/1.44 times from 20$^o$C to 40$^o$C, while they increased by a factor of 1.09/1.04/1.06 times in the range of 30–37$^o$C. Changes in these axonal excitability parameters increased especially rapidly at 42$^o$C. The strength-duration time constants for the normal/ALS1/ALS2 cases decreased by a factor of 8.77/4.74/1.68 times, while the rheobase currents for the same cases increased by a factor of 4.35/2.57/1.79 times, with a temperature increase from 20$^o$C to 42$^o$C. The significant changes in the rheobase currents in the range of 20–42$^o$C can be attributed to the higher threshold stimulus currents in the corresponding cases, as can be seen from their strength-duration curves (Fig. 1, first column).

### 3.2. *Recovery cycle abnormalities in the range of 20–42$^o$C for the normal and three ALS cases*

Absolute temperature-dependent recovery cycles of the normal, ALS1, ALS2, and ALS3 cases are plotted in Fig. 4 on logarithmic $x$-axes and linear $y$-axes. The horizontal lines in the panel figures indicate the threshold current (i.e. suprathreshold current increased by 5% of threshold) of conditioning stimuli. To clarify presentation, the recovery cycles and the control threshold currents of their corresponding conditioning stimuli are numbered from 1 to 6 and each consecutive number corresponds to temperatures of 20$^o$C, 30$^o$C, 34$^o$C, 37$^o$C, 40$^o$C and 42$^o$C, respectively. Recovery cycles are given for hypothermia (Fig. 4, 20$^o$C–curves 1), the physiological temperature range (Fig. 4, 30$^o$C–curves 2, 34$^o$C–curves 3, and 37$^o$C–curves 4), and during hyperthermia (Fig. 4, 40$^o$C–curves 5 and 42$^o$C–curves 6). The data comparing two temperatures (20$^o$C and 30$^o$C in Fig. 4, first row; 34$^o$C and 37$^o$C in Fig. 4, second row; 40$^o$C and 42$^o$C in Fig. 4, last row) are given in each panel figure for the normal and three ALS cases. The dotted curves and lines indicate the lower of the two temperatures. The presented data clearly show the complex effect of temperature on the conditioning control threshold current for the normal and three ALS cases. First, this current decreased with a temperature increase from 20$^o$C to 30$^o$C for the normal and abnormal cases. It then slightly increased for the normal and ALS1 cases and then slightly decreased for the ALS2 and ALS3 cases in the physiological temperature range of 34–37$^o$C. Finally, the threshold current increased rapidly during hyperthermia, especially at 42$^o$C, where it was large for the ALS1 case and largest for the normal case.

The absolute refractory period, relative refractory period, and axonal superexcitability in the 100 ms recovery cycle changed with increased temperature. The absolute refractory periods in the normal/ALS1/ALS2/ALS3 cases were 4.0/4.0/5.0/5.0, 2.8/2.8/2.9/2.9, 2.5/2.5/2.7/2.7, 2.4/2.4/2.5/2.5, 2.1/2.1/2.1/2.1 and 2.1/2.1/2.1/2.1 ms at 20$^o$C, 30$^o$C, 34$^o$C, 37$^o$C, 40$^o$C and 42$^o$C, respectively. Consequently, these periods were longest in the ALS2 and ALS3 cases during hypothermia, especially at 20$^o$C, and shortest during hyperthermia. The post-stimulus artifact (testing $V(t)$) relaxes back to the normal resting axonal membrane potential during the absolute refractory period. The related refractory period (i.e. the period after the conditioning action potential during which the threshold current of the test stimulus is elevated) was also different for the normal and abnormal cases. For the normal case, this period increased during hypothermia, especially at 20$^o$C, then decreased slightly for the physiological temperature range (30–37$^o$C). It again increased during hyperthermia, especially at 42$^o$C and after then decreased rapidly at 40$^o$C (Fig. 4, first column). The refractoriness (i.e. the increase in threshold current during the relative refractory period) was highest at the lowest temperature (20$^o$C) for the normal case. This refractoriness gradually decreased as the temperature increased from 30$^o$C to 37$^o$C. It then increased during hyperthermia. Compared with the normal case, refractoriness was reduced in the ALS1 case for temperatures ranging from 20$^o$C to 42$^o$C. For the same temperature range, there was no relative refractory period for the ALS2 and ALS3 cases (Fig. 4, third and last columns).

For the normal and ALS1 cases with increased temperature, the axonal superexcitability decreased during hypothermia and increased

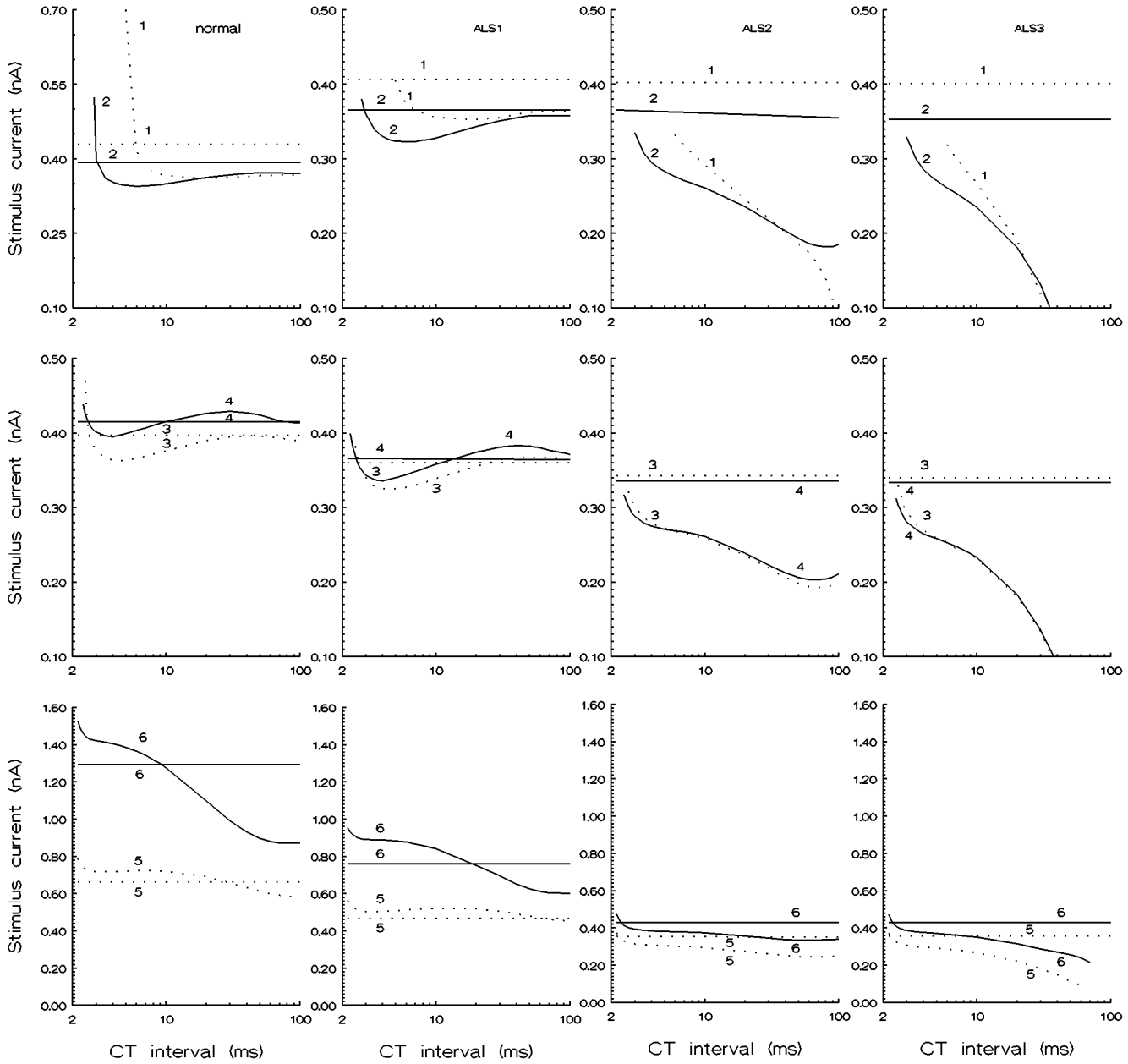


Fig. 4. Comparison between the absolute recovery cycles in the normal (first column), ALS1 (second column), ALS2 (third column), and ALS3 (last column) cases. The recovery cycles are numbered from 1 to 6 and each consecutive number corresponds to 20$^o$C, 30$^o$C, 34$^o$C, 37$^o$C, 40$^o$C and 42$^o$C, respectively. The recovery cycles are given in the temperature ranges of 20–30$^o$C (first row), 34–37$^o$C (second row) and 40–42$^o$C (last row). The *dotted* curves and lines indicate the lower of the two temperatures. The *horizontal* lines indicate the control threshold current (i.e. suprathreshold current increased by 5% of threshold) of the conditioning stimulus. CT intervals are plotted on logarithmic *x*-axis scales.

rapidly during hyperthermia. Also, the superexcitability period was followed by a late subexcitability period when the temperature was 37$^o$C (Fig. 4, curves 4). Unexpectedly, the axonal superexcitability increased rapidly in the ALS2 case at 20$^o$C and a block of each test stimulus applied at the end of recovery cycle was obtained (Fig. 4, curve 1). This axonal superexcitability decreased with the increase of temperature from 30$^o$C to 42$^o$C, but a late axonal subexitability was not obtained until the end of 100 ms recovery cycles (Fig. 4, third column). However, the axonal superexcitability increased rapidly in the ALS3 case, and a block of each test stimulus applied beyond the given CT intervals was obtained for temperatures from 20$^o$C to 42$^o$C (Fig. 4, last column).

The recovery cycles commented on above are normalized and presented together in Fig. 5. Each recovery cycle in the normal and abnormal cases for the given temperature is normalized to the control threshold current of its corresponding conditioning stimulus. The presented panel figures clearly show that the profile of recovery cycles is similar for the normal and ALS1 cases (Fig. 5, first row), and that the axonal superexcitabilities increase rapidly in the ALS2 case at 20$^o$C (Fig. 5, last row on the left) and in the ALS3 case for

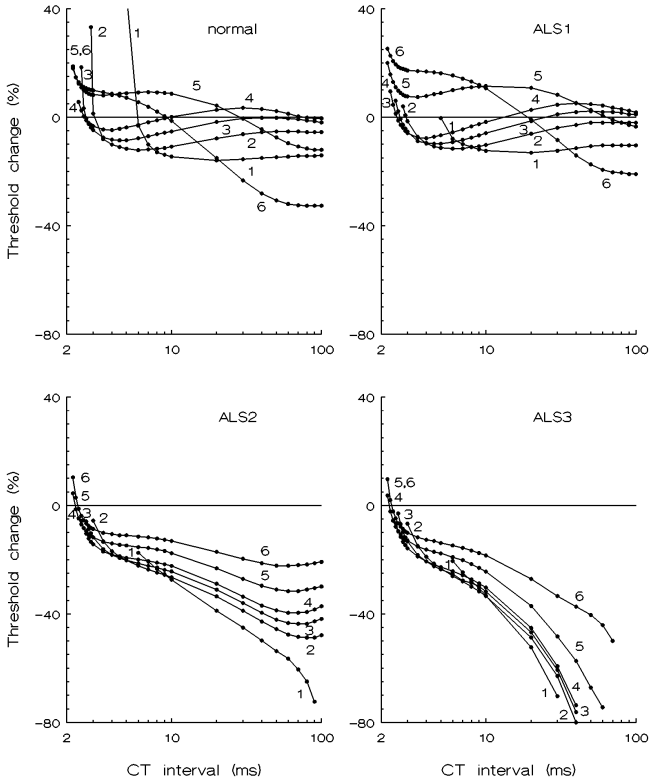


Fig. 5. Comparison between the normalized recovery cycles in the normal, ALS1, ALS2 and ALS3 cases. The recovery cycles are numbered from 1 to 6 and each consecutive number corresponds to 20$^o$C, 30$^o$C, 34$^o$C, 37$^o$C, 40$^o$C and 42$^o$C, respectively. For all cases, the *y*-axis is defined as 100 x $(I_{test} - I_{cond})/I_{cond}$ (%), where $I_{test}$ (nA) is the threshold current of the test stimulus and $I_{cond}$ (nA) is the control threshold current (i.e., suprathreshold current increased by 5% of threshold) of the conditioning stimulus. CT intervals are plotted on logarithmic *x*-axis scales.

temperatures from 20$^o$C to 42$^o$C (Fig. 5, last row on the right).

Recovery cycles depend not only on the temperature, but also on the regenerative axonal membrane depolarization or hyperpolarization caused by the conditioning afterpotential and could be explained by the delay-dependent testing potential. The temporal distributions of testing potentials for the normal, ALS1, ALS2, and ALS3 cases as a function of CT intervals are given during hypothermia and hyperthermia (Fig. 6). During hypothermia at 20$^o$C, the generated testing potentials for the different cases are given at moments corresponding to 99 ms (normal, ALS1, ALS2) and 39 ms (ALS3) CT intervals. For the normal and ALS1 cases, the conditioning afterpotentials were near the normal resting membrane potential (−86.7 mV) and the testing potentials were normal at the end of 100 ms recovery cycles. However, these afterpotentials increased rapidly at 97 ms and 35 ms in the ALS2, and ALS3 cases, respectively, and the test stimuli applied at 99 ms and 39 ms CT intervals were blocked (Fig. 6, first row). During hyperthermia at 40$^o$C and 42$^o$C, the generated testing potentials are given at moments corresponding to 69 ms and 79 ms CT intervals, respectively, for the normal, ALS1, ALS2, and ALS3 cases (Fig. 6, second and last rows). In the normal and ALS1 cases with increased temperature, the conditioning afterpotentials decreased to the normal resting potential and then became hyperpolarized, whereas the testing action potentials were similar. Also, during hyperthermia, the depolarizing conditioning afterpotentials increased slightly in the ALS2 case and the testing action potentials exhibited reduced amplitude. However, in the ALS3 case at 40$^o$C, the depolarizing conditioning afterpotential increased rapidly and oscillations of the generated testing action potential were obtained after application of the test stimulus at 69 ms CT interval (Fig. 6, second row). In this ALS3 case at 42$^o$C, the test stimulus applied at 79 ms CT interval was blocked as a result of the spontaneous axonal activity caused by the conditioning action potential (Fig. 6, last row).

The temporal distributions of testing potentials for the normal, ALS1, ALS2, and ALS3 cases as a function of CT intervals are also presented for the physiological temperature range at 30$^o$C, 34$^o$C, and 37$^o$C (Fig. 7). For the normal and the three ALS cases, the generated testing potentials are given at moments corresponding to 49 ms CT intervals for all temperatures, except in the case of ALS3 at 37$^o$C, where they are given at the moment corresponding to a 55 ms CT interval. Also, the testing action potentials are compared with the spontaneous membrane activities caused by the conditioning action potential in the ALS3 case (Fig. 7, last column). In the physiological temperature range, the testing potentials were near normal for the ALS1 case, but exhibited reduced amplitudes in the ALS2 case. However, for the ALS3 case, each test stimulus (applied at 49, 49, and 55 ms CT intervals at 30$^o$C, 34$^o$C, and 37$^o$C, respectively) was blocked as a result of the spontaneous axonal activities caused by the conditioning action potential.

## 4. Discussion

Simulated excitability indices were studied, such as strength-duration time constants, rheobase currents, and recovery cycles of the ALS1, ALS2, and ALS3 cases during hypothermia, hyperthermia, and in the physiological temperature range. These parameters were compared to those of the normal case. The results presented here, as well as those from both clinical [20–27] and previous studies [28, 29], conducted at normal temperature, showed that compared to the normal case, there is a characteristic: (i) longer strength-duration time constant and lower rheobase current, (ii) less refractoriness, and (iii) greater axonal superexcitability and reduced late subexcitability. Nevertheless, in the three ALS cases the strength-duration time constants gradually decreased with increased temperature from 20$^o$C to 42$^o$C. They were longer than those of the normal case. There was also a reciprocal relationship between the temperature-dependent strength-duration time constants and rheobase currents. These excitability parameters were more sensitive to hyperthermia, especially at 42$^o$C, than at temperatures in the physiological range of 30–37$^o$C. However, the equivalent strength-duration time constants and rheobase currents obtained for the ALS2 and ALS3 cases showed that the blockage of internodal slow potassium channels does not contribute to these excitability parameters. The results presented here also confirmed that recovery cycle profiles were similar for the normal and ALS1 cases across the whole temperature range. Axonal superexcitability increased with temperature decreases in the ALS2 case, and each test stimulus applied at the end of the 100 ms recovery cycle was blocked at the lowest temperature tested (20$^o$C). Increased axonal superexcitability was not recovered for the ALS3 case during hypothermia, hyperthermia, and for the physiological temperature range, and each test stimulus applied beyond a given CT interval was blocked. This blockage resulted from spontaneous axonal activities caused by the conditioning (first) stimulus. However, the different recovery cycles

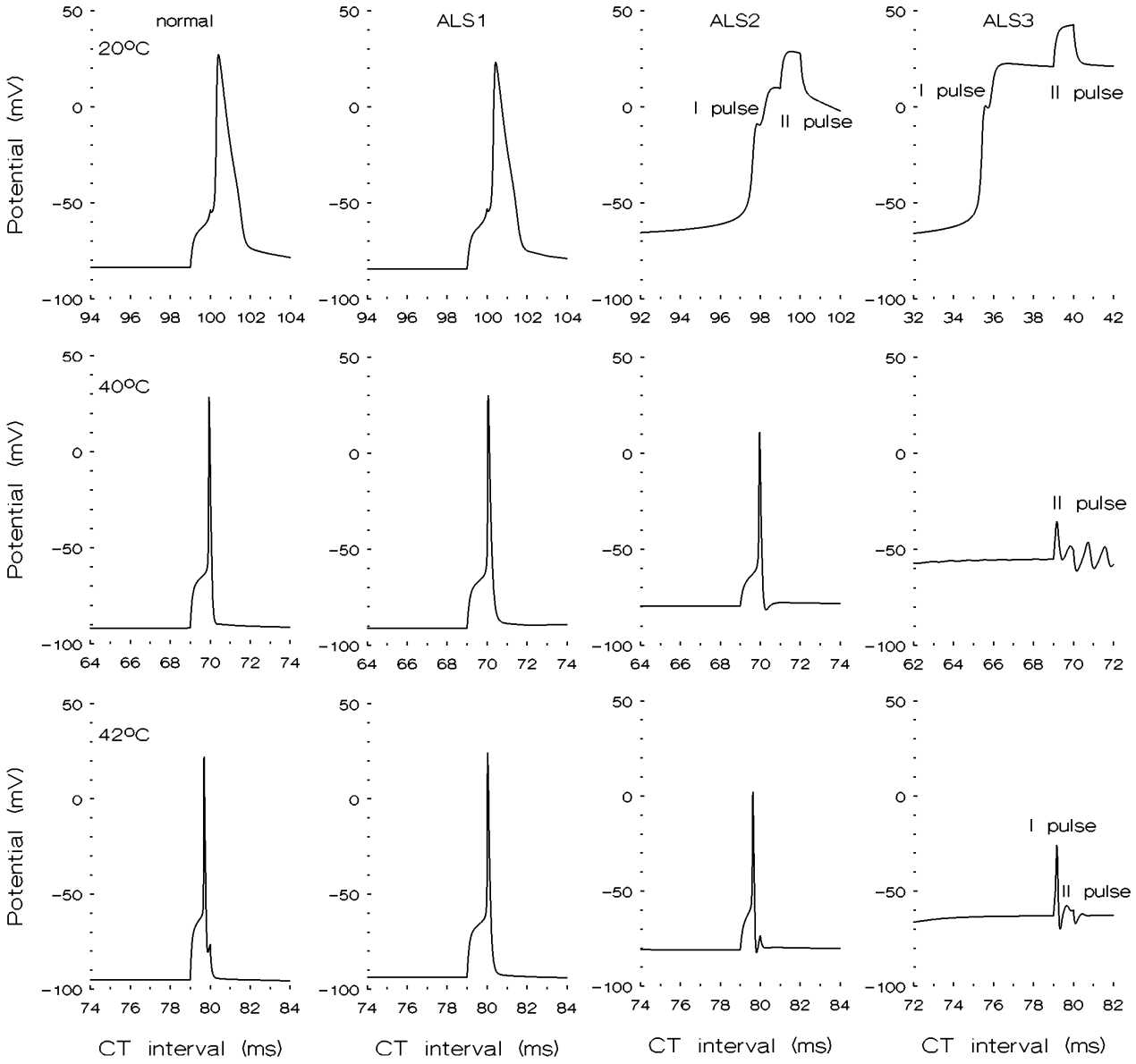


Fig. 6. Temporal distributions of action potentials when the test stimulus is applied as a function of CT interval, corresponding to: CT = 99 ms for the normal, ALS1, and ALS2 cases and CT = 39 ms for the ALS3 case during hypothermia at 20$^o$C (first row); CT = 69 ms and CT = 79 ms for the normal, ALS1, ALS2 and ALS3 cases during hyperthermia at 40$^o$C (second row) and 42$^o$C (last row), respectively. The testing action potentials are compared with spontaneous axonal activity caused by the conditioning action potentials in the ALS2 case at 20$^o$C and in the ALS3 case (last column). The action potentials are presented at each node from the 7th to the 14th and at each internodal segment between them. However, these segments respond equally, as periodic fibre polarization is realized and an overlap of the potentials in the nodal and internodal segments is obtained.

obtained for the ALS2 and ALS3 cases show that the blockage of internodal slow potassium channels mainly contributes to this excitability parameter. The resulting superexcitability axonal activities of the nodal and internodal axolemma beneath the myelin sheath, caused by spontaneous discharges based on the continuous activation and reactivation of ion (mainly "transient" $Na^+$) channels in these compartments can be regarded as a prelude to neuronal death.

## 5. Conclusion

As suggested from simulation results, it is proposed that the temperature-dependent strength-duration time constants, rheobase currents, and recovery cycles in the three ALS cases can be clinically interpreted as specific indicators for the motor neuron disease ALS. Results obtained are essential for the interpretation of mechanisms of excitability parameter measurements in healthy and ALS patients with symptoms of cooling, warming and fever, which can result from alteration in body temperature.

## Acknowledgments

We thank the Institute of Biophysics and Biomedical Engineering for use of computational facilities.

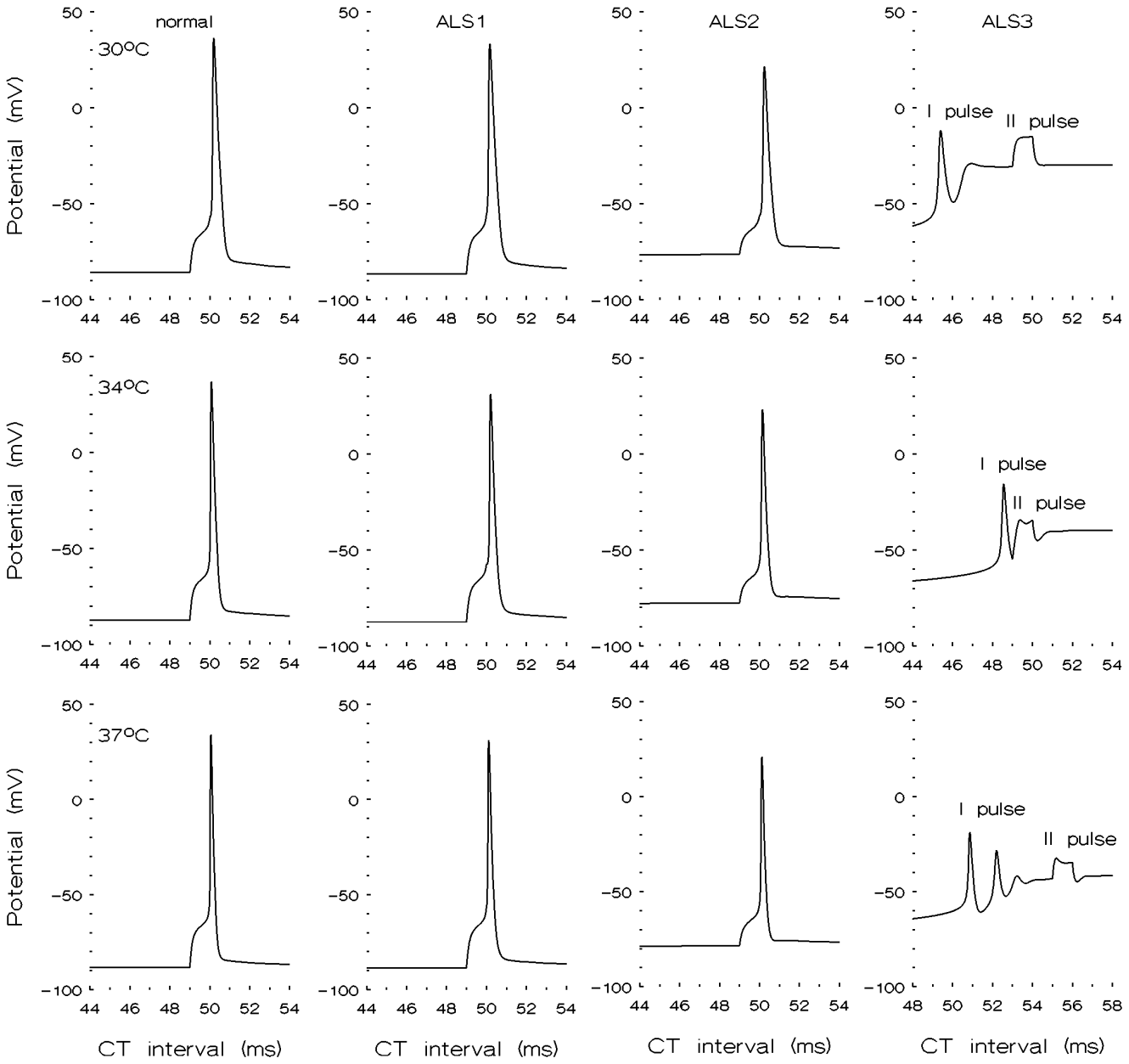


Fig. 7. Temporal distributions of action potentials when the test stimulus is applied as a function of the CT intervals, corresponding to: CT = 49 ms for the normal, ALS1, ALS2, and ALS3 cases in the physiological temperature range at 30$^o$C (first row), 34$^o$C (second row) and 37$^o$C (last row), respectively, except for the ALS3 case, where the CT = 55 ms at 37$^o$C. The testing potentials are compared with spontaneous axonal activities caused by the conditioning action potentials in the ALS3 case (last column). The action potentials are presented at each node from the 7th to the 14th and at each internodal segment between them. However, these segments respond equally, as periodic fibre polarization is realized and an overlap of the potentials in the nodal and internodal segments is obtained.

## Conflict of Interest

All authors declare no conflict of interest.

## References

[1] Desai J and Swash M (2002) Essentials of diagnosis. In, Kuncl WR (eds.) *Motor Neuron Disease* (pp. 1-21). London, WB Saunders.

[2] Finsterer J (2006) Familiar Amyotrophic Lateral Sclerosis. In, Murray CA (eds.) *Amyotrophic Lateral Sclerosis: New Research* (pp. 1-49). New York, Nova Science Publishers, Inc..

[3] Rowland LP and Shneider NA (2001) Amyotrophic lateral sclerosis. *The New England Journal of Medicine* **344(22)**, 1688-1700.

[4] De Carvalho M and Swash M (2013) Origin of fasciculations in amyotrophic lateral sclerosis and benign fasciculation syndrome. *JAMA Neurology* **70(12)**, 1562-1565.

[5] Daube JR (2000) Electrodiagnostic studies in amyotrophic lateral sclerosis and other motor neuron disorders. *Muscle & Nerve* **23(10)**, 1488-1502.

[6] Finsterer J, Fuglsang-Frederiksen A and Mamoli B (1997) Needle EMG of the tongue: motor unit action potential versus peak ratio analysis in limb and bulbar onset amyotrophic lateral sclerosis. *Journal of Neurology, Neurosurgery & Psychiatry* **63(2)**, 175-180.

[7] Kuwabara S, Shibuya K and Misawa S (2014) Fasciculations, axonal hyperexcitability, and motoneuronal death in amyotrophic lateral sclerosis. *Clinical Neurophysiology: Official Journal of the International Federation of Clinical Neurophysiology* **125(5)**, 872-873.

[8] Layzer RB (1994), The origin of muscle fasciculation and cramps. *Muscle & Nerve* **17(11)**, 1243-1249.

[9] Roth G (1982) The origin of fasciculations. *Annals of Neurology* **12(6)**, 542-547.

[10] Roth G (1984) Fasciculations and their F-response: Localization of their axonal origin. *Journal of the Neurological Sciences* **63(3)**, 299-306.

[11] Rowinska-Marcinska K, Ryniewicz B, Hansmanowa-Petrusewicz I and Karvanska A (1997) Diagnostic values of satellite potentials in clinical EMG. *Electromyography and Clinical Neurophysiology* **37(8)**, 483-489.

[12] Trojaborg W and Buchthal F (1965) Malignant and bening fasciculations. *Acta Neurologica Scandinavica* **41(S13)**, 251-254.

[13] Guiloff RJ and Modarres-Sadeghi H (1992) Voluntary activation and fiber density of fasciculations in motor neuron disease. *Annals of Neurology* **31(4)**, 416-424.

[14] Bostock H (1995) Mechanisms of accommodation and adaptation in myelinated axons. In, Waxman SG et al. (eds.) *The Axon* (pp. 311-327). New York, Oxford University Press.

[15] Bostock H and Baker M (1988) Evidence for two types of potassium channel in human motor axons in vivo. *Brain Research* **462(2)**, 354-358.

[16] Bostock H, Cikurel K and Burke D (1998) Threshold tracking techniques in the study the human peripheral nerve. *Muscle & Nerve* **21(2)**, 137-158.

[17] Burke D, Kiernan MC and Bostock H (2001) Excitability of human axons. *Clinical Neurophysiology : Official Journal of the International Federation of Clinical Neurophysiology* **112(9)**, 1575-1585.

[18] Bostock H (1983) The strength-duration relationship for excitation of myelinated nerve: computed dependence on membrane parameters. *Journal of Physiology (London)* **341(1)**, 59-74.

[19] Mogyoros I, Kiernan MC and Burke D (1996) Strenth-duration properties of human peripheral nerve. *Brain* **119(Pt2)**, 439-447.

[20] Bostock H, Sharief MK, Reid G and Murray NM (1995) Axonal ion channel dysfunction in amyotrophic lateral sclerosis. *Brain* **118(Pt1)**, 217-225.

[21] Iwai Y, Shibuya K, Misawa S, Sekiguchi Y, Watanabe K, Amino H and Kuwabara S (2016) Axonal dysfunction precedes motor neuronal death in amyotrophic lateral sclerosis. *Plos One* **11(7)**, e0158596.

[22] Mogyoros I, Kiernan MC, Burke D and Bostock H (1998) Strenth-duration properties of sensory and motor axons in amyotrophic lateral sclerosis. *Brain* **121(Pt5)**, 851-859.

[23] Menon P, Kiernan MC and Vucic S (2014) ALS pathophysiology: Insights from the split-hand phenomenon. *Clinical Neurophysiology* **125(1)**, 186-193.

[24] Nakava M, Kuwabara S, Kanai K, Misawa S, Tamura N, Sawai S, Hattori T and Bostock H (2006) Distal excitability changes in motor axons in amyotrophic lateral sclerosis. *Clinical Neurophysiology* **117(7)**, 1444-1448.

[25] Park B, Lin CS-Y and Kiernan MC (2017) Axonal excitability: molecular basis and assessment in the clinic. In, Mills KR (eds.) *Oxford Textbook of Clinical Neurophysiology* (pp. 97-106). Oxford, Oxford University Press.

[26] Shibuta Y, Nodera H, Nodera A, Okita T, Asanuma K, Izumi Y and Kaji B (2010) Utility of recovery cycle with two conditioning pulses for detection of impaired axonal slow potassium current in ALS. *Clinical Neurophysiology* **121(12)**, 2117-2120.

[27] Vucic S and Kiernan C (2006) Axonal excitability properties in amyotrophic lateral sclerosis. *Clinical Neurophysiology* **117(7)**, 1458-1466.

[28] Stephanova DI (2006) Excitability and potentials of human fibres in amyotrophic lateral sclerosis: model investigations. In, Murray CA (eds.) *Amyotrophic Lateral Sclerosis: New Research* (pp. 155-178). New York, Nova Science Publishers Inc..

[29] Stephanova DI and Dimitrov B (2013) Simulated demyelinating neuropathies and neuronopathies. In, Stephanova DI and Dimitrov B (eds.) *Computational Neuroscience: Simulated Demyelinating Neuropathies and Neuronopathies*(pp. 33-93). Boca Raton, London, New York, CRC Press.

[30] Stephanova DI and Daskalova M (2014) Theoretical predication of the effects of temperature on simulated adapted processes in human motor nerve axons at $20^oC-42^oC$. *Journal of Integrative Neuroscience* **13(3)**, 529-543.

[31] Stephanova DI (2001) Myelin as longitudinal conductor: A multilayered model of the myelinated human motor nerve fibre. *Biological Cybernetics* **84(4)**, 301-308.

[32] Stephanova DI and Dimitrov B (2013) Models and methods for investigation of the human motor nerve fibre. In, Stephanova DI and Dimitrov B (eds.) *Computational Neuroscience: Simulated Demyelinating Neuropathies and Neuronopathies* (pp. 18-32), Boca Raton, London, New York, CRC Press.

[33] Stephanova DI, Daskalova M and Krustev SM (2013) Modified multilayered model of temperature dependent motor nerve axons. *Scripta Scientifica Medica* **45(3)**, 36-41.

[34] Stephanova DI and Kossev A (2016) Theoretical predication of temperature effect on conducting processes in simulated amyotrophic lateral sclerosis at $20\text{-}42^oC$, *Journal of Integrative Neuroscience* **15(2)**, 261-276.

[35] Stephanova DI and Daskalova M (2014) Effects of temperature on simulated electrotonic potentials and their current kinetics of human motor nerve axons at $20^oC-42^oC$. *Journal of Integrative Neuroscience* **13(3)**, 447-467.

[36] Stephanova DI and Bostock H (1996) A distributed-parameter model of the myelinated human motor nerve fibre: Temporal and spatial distributions of electrotonic potential and ionic currents. *Biological Cybernetics* **74(6)**, 543-547.